






RESEARCH ARTICLE

Elucidating dynamic behavior of synthetic supramolecular polymers in water by hydrogen/deuterium exchange mass spectrometry

Xianwen Lou¹ | Sandra M. C. Schoenmakers¹ | Joost L. J. van Dongen¹ | Miguel Garcia-Iglesias^{2,3}  | Nicolás M. Casellas² | Marcos Fernández-Castaño Romera^{4,5}  | Rint P. Sijbesma⁴  | E. W. Meijer¹  | Anja R. A. Palmans¹ 

¹Department of Chemical Engineering and Chemistry, Institute for Complex Molecular Systems, Eindhoven University of Technology, Eindhoven, The Netherlands

²Department of Organic Chemistry, Universidad Autónoma de Madrid (UAM), Madrid, Spain

³Department of Chemistry and Process & Resource Engineering, University of Cantabria, Santander, Spain

⁴Department of Chemical Engineering and Chemistry, Eindhoven University of Technology, Eindhoven, The Netherlands

⁵SupraPolix BV, Eindhoven, The Netherlands

Correspondence

Anja R. A. Palmans, Department of Chemical Engineering and Chemistry, Institute for Complex Molecular Systems, Eindhoven University of Technology, P. O. Box 513, 5600 MB, Eindhoven, The Netherlands.

Email: a.palmans@tue.nl

Funding information

MINECO, Spain, Grant/Award Number: IJCI-2015-252389; Marie Curie FP7 SASSYPOL ITN program, Grant/Award Number: 607602; European Research Council, Grant/Award Number: 788618; Dutch Ministry of Education, Culture and Science, Grant/Award Number: 024.001.035

Abstract

A comprehensive understanding of the structure, self-assembly mechanism, and dynamics of one-dimensional supramolecular polymers in water is essential for their application as biomaterials. Although a plethora of techniques are available to study the first two properties, there is a paucity in possibilities to study dynamic exchange of monomers between supramolecular polymers in solution. We recently introduced hydrogen/deuterium exchange mass spectrometry (HDX-MS) to characterize the dynamic nature of synthetic supramolecular polymers with only a minimal perturbation of the chemical structure. To further expand the application of this powerful technique some essential experimental aspects have been reaffirmed and the technique has been applied to a diverse library of assemblies. HDX-MS is widely applicable if there are exchangeable hydrogen atoms protected from direct contact with the solvent and if the monomer concentration is sufficiently high to ensure the presence of supramolecular polymers during dilution. In addition, we demonstrate that the kinetic behavior as probed by HDX-MS is influenced by the internal order within the supramolecular polymers and by the self-assembly mechanism.

Xianwen Lou and Sandra M. C. Schoenmakers contributed equally to this study.

This is an open access article under the terms of the Creative Commons Attribution-NonCommercial License, which permits use, distribution and reproduction in any medium, provided the original work is properly cited and is not used for commercial purposes.

© 2021 The Authors. *Journal of Polymer Science* published by Wiley Periodicals LLC.

KEYWORDS

cryoTEM, exchange dynamics, hydrogen deuterium exchange, self-assembly, supramolecular chemistry, supramolecular polymers

1 | INTRODUCTION

Supramolecular assemblies in water attract a great deal of interest because a plethora of different types of morphologies can be formed depending on the molecular structure of the monomer.^{1–3} Particularly promising are one-dimensional fibrillar synthetic structures that can be applied as synthetic biomaterials due to their resemblance to natural fibrillar assemblies and their modularity, which permits the introduction of a variety of functional groups.^{4–12} Both the formation mechanism of the assemblies as well as the rate of the dynamic exchange of monomers between the assemblies has been used as a handle to tune the functions of the formed superstructures.^{13–15} In fact, the dynamic behavior of supramolecular systems can be tuned to match the inherent dynamic behavior of the supramolecular interactions in living tissues.^{16–18} A fundamental understanding of the structure, mechanism of self-assembly and the dynamic behavior are therefore essential for the creation of such intricate biomaterials.

Understanding the interplay between molecular structure, formation mechanism, and dynamic exchange is important to guide the application potential of 1D fibrillar assemblies in adaptive biomaterials. As a result, it is important to evaluate these properties simultaneously without changing the nature of the supramolecular assemblies. Microscopy techniques such as cryogenic transmission electron microscopy (cryoTEM) are available that visualize on nanometer length scales the morphologies formed by supramolecular systems close to their native state.^{19,20} In addition, spectroscopy techniques such as UV–Vis and CD spectroscopy allow to elucidate the mechanism with which monomers form supramolecular polymers in solution.²¹ In contrast, analytical methods that accurately quantify the dynamic behavior of a monomer exchanging between polymers, or the movement of a monomer along a polymer chain, typically require the attachment of molecular probes to the monomer of interest, such as spin labels or fluorescent dyes.^{22–26} These probes are often rather bulky, which may have a significant influence on the local intermolecular interactions and may change the hydrophobic/hydrophilic balance within the monomer. As a result, the solubility and dynamic behavior of the monomer with the probe attached may be significantly altered compared to the “bare” monomer.

To avoid the need for molecular probes that change the monomer's character, we started to explore hydrogen/deuterium exchange mass spectrometry (HDX-MS) for tracking the dynamic behavior of supramolecular polymers in water.²⁷ HDX-MS is a key technique for studying the structural and dynamic aspects of proteins.^{28–36} Hydrogen atoms in OH, NH, and SH groups are labile and can exchange with labile hydrogen atoms of the surrounding solvent. Whereas the exchange of H to H is undetectable, exposing molecules with labile hydrogen atoms to a D₂O environment will lead to H to D replacements that increase the mass of the molecule by one unit per exchange event. The rate of molecular mass increase can be accurately monitored by mass spectrometry (MS). In the case of proteins, amide hydrogen atoms exhibit rapid exchange rates if they are accessible to the solvent but show reduced exchange rates if they are hydrogen bonded and/or buried in hydrophobic regions. It is nowadays possible to obtain HDX structural resolution close to the amino acid level and to elucidate protein dynamics.^{37–40} Additionally, HDX-MS has been used to reveal the mechanism of assembly and to quantify the rate constants of growth and disassembly of amyloid fibrils in solution.^{41,42}

Schalley et al adapted HDX-MS to study supramolecular systems, and found that hydrogen bonding was important for the organization of the building blocks.^{43–45} Inspired hereby, we applied HDX-MS to elucidate the dynamic behavior of benzene-1,3,5-tricarboxamide (BTA)-based supramolecular polymers in water.²⁷ Although the HDX processes for supramolecular polymers and for proteins share a lot of similarities, they also have some important differences. Most notably, the HDX events in proteins are generally mediated by conformational fluctuations without changing the primary structure of the proteins, whereas H/D exchange in supramolecular assemblies occurs after the release of a monomer into the solution. Accordingly, experimental aspects which have been optimized and widely accepted in HDX-MS for protein samples need to be re-evaluated for supramolecular polymers.

In this article, we apply previously studied BTA-based supramolecular polymers in water^{27,46} to first address key experimental aspects of HDX-MS for supramolecular polymers, namely the choice of the MS method, and the effect of dilution on the HDX-MS analysis. We also devise an analysis method to quantify the abundances of all deuterated species as a function of time. Then, we compare the dynamic behavior of **BTA (1)** (Scheme 1) to that

of three other supramolecular monomers that polymerize via different formation mechanisms, cooperative or isodesmic, and form intrinsically different morphologies as revealed by cryoTEM. We recently elucidated that **BTA** (**1**) forms a double helical structure in water.⁴⁷ In contrast, diacetylene bis-urea amphiphile (**BU** [**2**]) forms fibrous bundles,⁴⁸ and the two benzotrithiophenes (**BTT-5F** [**3**] and **BTT** [**4**]) form single fibers (Scheme 1).¹³ **BTT-5F** (**3**) polymerizes via an isodesmic mechanism, whereas all other monomers polymerize via a cooperative mechanism. We find that there is a correlation between the rate and degree of H/D exchange, the formation mechanism and the formed morphology. All in all, we conclude that HDX-MS is applicable to all supramolecular polymers in water, as long as there are exchangeable hydrogens protected from direct contact with water in the polymer and the monomer concentration is sufficient to ensure the presence of supramolecular polymers during the H/D exchange in the solution.

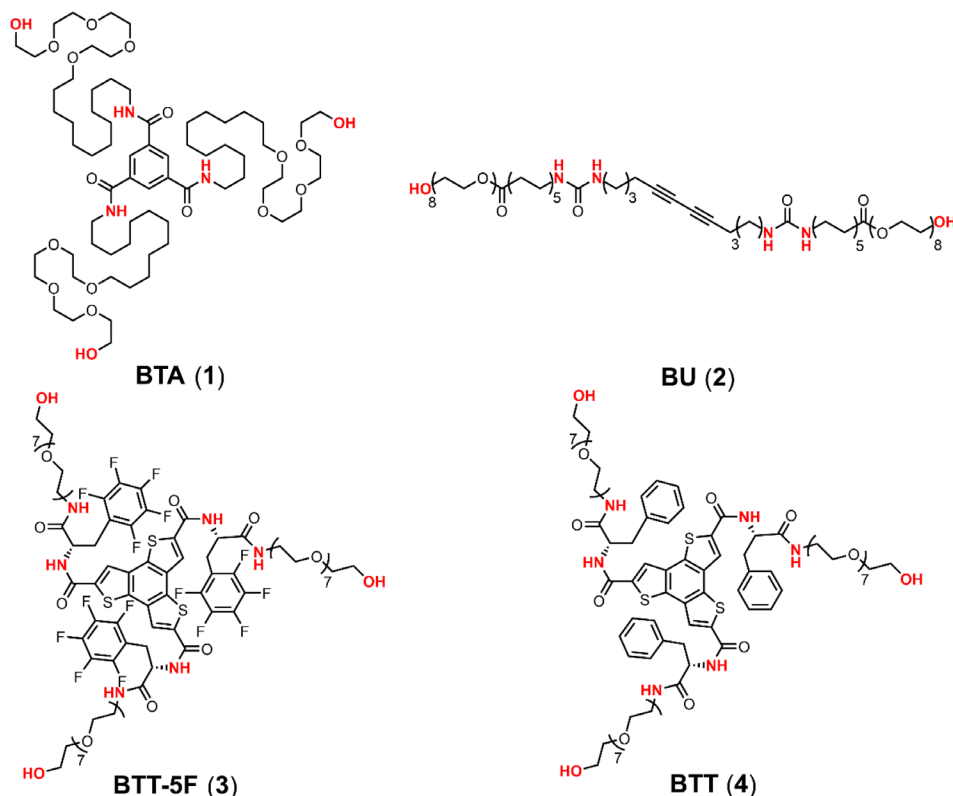
2 | RESULTS AND DISCUSSION

2.1 | Experimental aspects of HDX-MS in synthetic supramolecular polymers

Before discussing the interplay between morphology, formation mechanism and dynamic behavior in the

compounds shown in Scheme 1, we first address some fundamental aspects of the HDX-MS analysis used in this work. The aim of this assessment is to ensure that HDX-MS can be widely and reliably used, and that the information obtained on exchange rates does not depend on the experimental parameters applied. For this purpose, we select the well-studied **BTA** (**1**), which contains six labile hydrogen atoms: three OH groups in the periphery and three NH groups in the core. Our previous results showed that dilution of a 500 μM **BTA** (**1**) solution in H_2O 100x into D_2O showed two distinct distributions corresponding to **BTA3D** and **BTA6D** when analyzed with ESI-MS. **BTA3D** is formed instantaneously upon dilution by the exchange of the three OH groups into three OD groups. **BTA6D** is formed over time as also the three labile NH hydrogen atoms get exchanged into NDs (Figure 1A).

ESI MS^{27,44} has been shown to be successful to track the exchange of H to D as a function of time in case of **BTA** (**1**), but we wondered if MALDI MS could also be applied. A detailed study using **BTA** (**1**) and the evaluation of a number of MALDI matrix materials revealed that in all experimental conditions the loss of deuterium as a result of back-exchange using MALDI MS was significantly higher than when using ESI MS (see ESI for details, Section 3). The ionization reactions in the MALDI plume generate substantial back-exchange, even when an aprotic matrix is used and great care is taken



SCHEME 1 Chemical structures of the supramolecular building blocks of **BTA** (**1**), **BU** (**2**), **BTT-5F** (**3**) and **BTT** (**4**).

Exchangeable hydrogen atoms are shown in red. BU, bis-urea amphiphile; BTA, benzene-1,3,5-tricarboxamide; BTT, benzotrithiophene [Color figure can be viewed at wileyonlinelibrary.com]

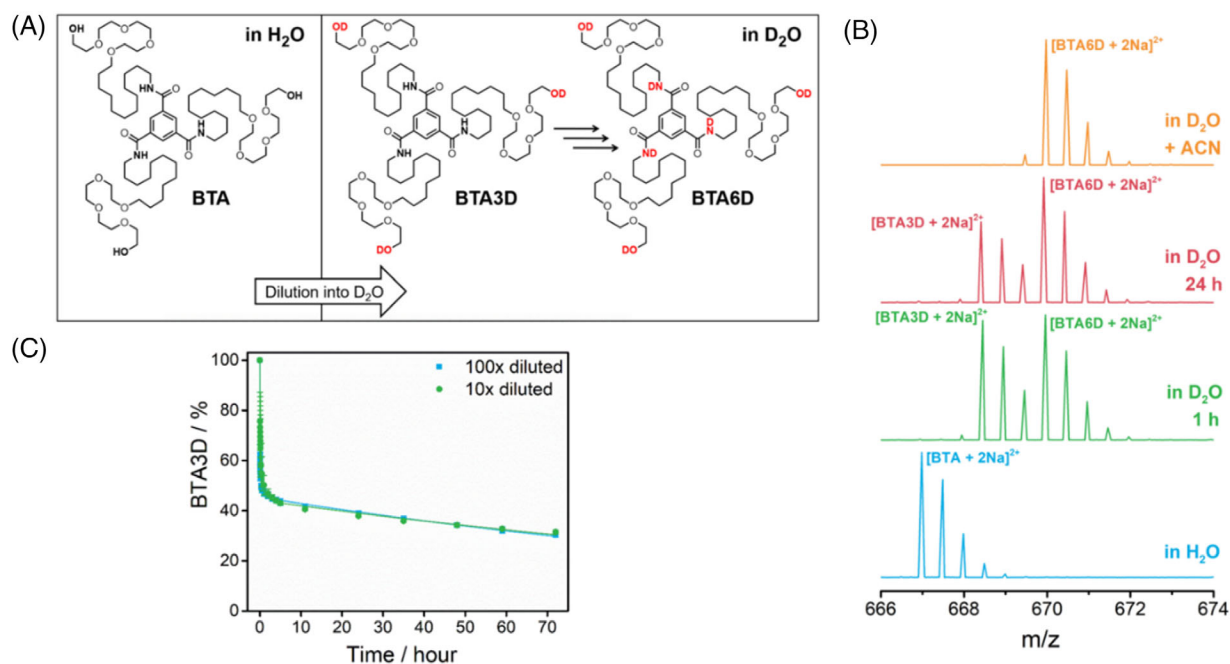


FIGURE 1 (A) Schematic representation of the HDX-MS process of **BTA (1)** including the chemical structures of BTA analogues before and after dilution in D₂O. (B) ESI-MS spectra of the doubly charged ions of **BTA (1)** after 100x dilution of a 500 μM sample. The sample was diluted into H₂O, D₂O or a 1/1 D₂O/ACN mixture. (C) HDX-MS curves of 500 μM samples of **BTA (1)** with different dilution procedures. Percentages of BTA3D over time with 100x dilution into D₂O (blue squares) and 10x dilution into D₂O (green circles) are plotted as function of time. Measurements were performed at room temperature, the error bars represent the standard deviation calculated from three separate experiments and lines are added to guide the eye. BTA, benzene-1,3,5-tricarboxamide; HDX-MS, hydrogen/deuterium exchange mass spectrometry [Color figure can be viewed at wileyonlinelibrary.com]

during the sample preparation process. Thus, we conclude that MALDI MS is less suitable than ESI MS for the HDX-MS analysis of the supramolecular polymers in water. This result is in line with findings for protein samples where also higher deuterium losses have been observed with MALDI than ESI.³³

A second important aspect of HDX-MS is to accurately extract the abundance of the differently deuterated species from the high-resolution MS spectra especially when remnant H₂O is present after dilution into D₂O. We therefore here devise a method to track the deuterated species over time and we will illustrate the calculations with **BTA (1)**. Figure 1(B) shows the MS spectra of **BTA (1)** after dilution in H₂O, D₂O and D₂O/acetonitrile. The latter solvent combination serves as a reference as **BTA (1)** is molecularly dissolved herein.⁴⁹ In fact, BTA6D and its isotopes is the dominant distribution observed after 100x dilution in D₂O/acetonitrile, indicating that when the BTAs are molecularly dissolved, all labile hydrogens are immediately exchanged. However, the small peak at m/z 669.48 is indicative for BTA5D which is there because of remnant H₂O after dilution. After 1 h in D₂O, the peak corresponding to BTA3D has the same intensity as the peak corresponding to BTA6D (green spectrum), and after 24 h the peak for BTA6D has

grown at the expense of the peak for BTA3D (red spectrum). The peaks between the monoisotopic peaks of BTA3D and BTA6D coincide with the isotope distribution of BTA3D and with artifacts introduced by D/H exchange of the deuterium atoms of BTA6D caused by a trace amount of H₂O present after the dilution. Therefore, we correct for the isotope distributions that overlap with the peaks of more deuterated BTAs and subtract the theoretical percentage of BTAs formed by remnant H₂O such that only the percentage of intermediates that truly originate from H/D exchange is presented (see ESI† Section 4 for details on the calculations). The result of the percentage of BTA3D as a function of time, corrected for small amounts of H₂O, is shown in Figure 1(C). It is very similar to the results we observed in the previous work.²⁷

Because of the non-covalent nature of the bonds holding supramolecular polymers together, the reduction in concentration by diluting a solution from H₂O to D₂O might affect the stability of the supramolecular polymers and thereby their dynamic behavior. Thus, an important experimental factor to take into consideration is if the degree of dilution of the sample into D₂O affects the exchange. We compared the distribution of BTA3D when diluting an aqueous 500 μM sample of **BTA (1)** 100x with that diluted 10x into D₂O. When a 10x dilution is used,

the MS spectra are more complicated and contain prominent distributions of BTA2D, BTA4D and BTA5D (Figure S1, ESI[†]), because the H₂O concentration is about 10 vol% and cannot be ignored. When the statistical distributions for D/H exchange are taken into account, (see ESI[†] section 4, Tables S2 and S3) the abundance of the deuterated species can accurately be calculated. Figure 1(C) shows that the BTA3D percentage of a 100x and 10x diluted sample shows no significant differences as a function of time. Interestingly, the same holds when 100x dilution is compared to two times 10x dilution (Figure S2 and S3, ESI[†]).

Finally, we observed for **BTA (1)** that 100x dilution of samples with different starting concentrations (1 mM, 0.5 mM or 0.1 mM, Figure S4, ESI[†]) does not affect the HDX exchange profile. The association constant in supramolecular polymers based on **BTA (1)** is very high and the critical aggregation concentration (CAC) is well below 5 μ M. Thus, as long as the final concentration is well above the CAC of the supramolecular polymer, the kinetic profiles are not affected by the start and end concentrations as long as the percentage of H₂O is taken into account during the analysis. When less stable systems are considered (as in the case of **BTT-5F (3)**, vide infra) care should be taken to ensure that the concentration is above the CAC to keep the molecules assembled after dilution into D₂O.

2.2 | Analysis of the HDX experiments of compounds 1–4

To enable a proper comparison of the HDX-MS results between compounds **1–4**, which all have different amounts of labile H atoms, all HDX data are visualized in such a way that we track the same kind of species as a function of time. In this way, the information on the internal order and H/D exchange mechanism can be extracted. We first show the percentage of all deuterated species of **BTA (1)** after 100x dilution into D₂O in the time-dependent HDX-MS experiments (Figure 2, see for details ESI Section 4). This method of plotting reveals that there is a small percentage of BTA4D and BTA5D in the beginning of the experiment (see zoom-in in Figure S5, ESI[†]) which was previously overlooked. After 1 h, the percentage of BTA4D and BTA5D has decreased and the H/D exchange is dominated by either by BTA3D or BTA6D.

Next, we study supramolecular assemblies based on diacetylene bis-urea amphiphiles (**BU [2]**). These linear molecules stack on top of each other via urea hydrogen bonding and hydrophobic interactions and associate laterally to form worm-like micelles in water.⁴⁸ **BU (2)** has

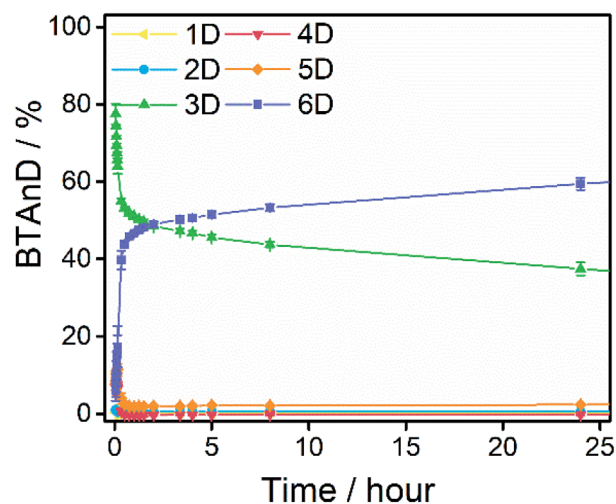


FIGURE 2 The percentage of the different deuterated analogues of **BTA (1)** as a function of time after the 100x dilution of an aqueous 500 μ M sample of **BTA (1)** into D₂O ($T = \text{room temperature}$). The lines are added to guide the eye. BTA, benzene-1,3,5-tricarboxamide [Color figure can be viewed at wileyonlinelibrary.com]

two peripheral OH atoms that are on the outside of the assemblies and are easily accessible for D₂O, which would lead to the formation of BU2D (Figure 3A). The four bis-urea NHs are not in direct contact with the solvent and form hydrogen bonds to allow for linear stacking.⁵⁰ Only BU6D is observed after 100x dilution in the presence of ACN, in which **BU (2)** is molecularly dissolved, since all interactions are broken and all NH and OH groups are immediately accessible for the solvent (Figure S6, ESI[†]). In contrast, after 1 h of H/D exchange in D₂O, BU2D and BU6D are the most abundant species in the ESI-SM spectra, whereas after 24 h BU6D is the major species and only a small amount of BU2D remains (Figure 3(B)).

The percentages of the intermediates BU1D, BU3D, BU4D, and BU5D alongside those of BU2D and BU6D, using the method discussed for **BTA (1)**, are shown in Figure 3(C). The results show that the percentage of BU2D rapidly decreases in the first 5 h, after which it stabilizes. The percentage of BU3D, BU4D and BU5D increases at the start of the experiment, until a maximum is reached and then the percentage decreases. The time needed to reach the maximum percentage increases with the number of deuterium labels that is incorporated: BU3D reaches its maximum after 10 min, BU4D after 30 min and BU5D after 1 h (see zoom-in in Figure S7, ESI[†]). After 8 h the contributions of BU3D, BU4D and BU5D remains constant and are almost negligible.

C₃-Symmetrical benzotrithiophenes (BTTs) (**3**) and (**4**) have similar molecular structures but because the

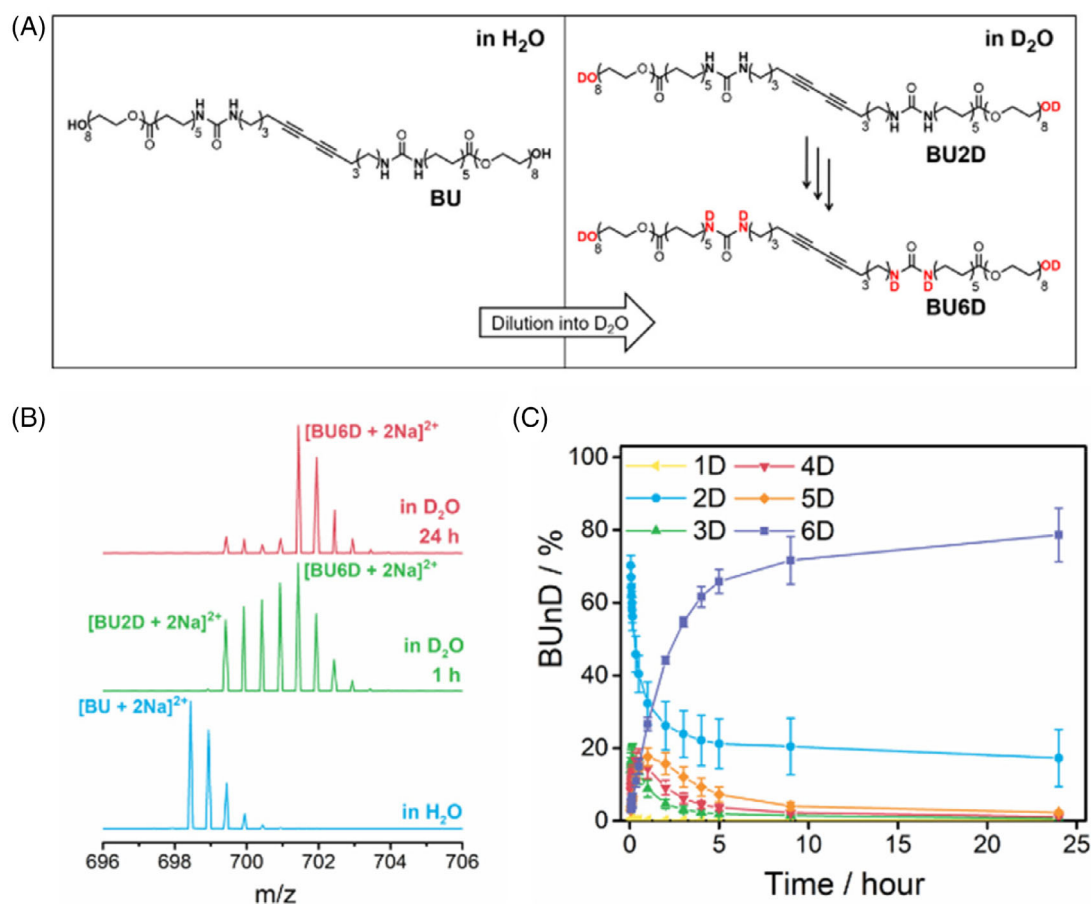


FIGURE 3 HDX-MS experiment of **BU** (**2**). (A) Schematic representation of the HDX-MS process including the chemical structures of the **BU** analogues before and after dilution in D_2O . (B) ESI-MS spectra of the doubly charged ions of **BU** (**2**) after 100x dilution of a 500 μM sample. The sample was diluted into H_2O or D_2O . (C) the percentages of the different deuterated analogues of **BU** (**2**) as a function of time after the 100x dilution of an aqueous 500 μM sample of **BU** (**2**) into D_2O ($T = \text{room temperature}$). The symbols represent the average and the error bars the standard deviation calculated from three independent measurements. The lines are added to guide the eye. **BU**, bis-urea amphiphile; HDX-MS, hydrogen/deuterium exchange mass spectrometry [Color figure can be viewed at wileyonlinelibrary.com]

hydrophobicity changes by replacing *L*-phenylalanine (**BTT** (**4**)) with *L*-pentafluorophenylalanine (**BTT-5F** (**3**)) the mechanism of self-assembly changes. **BTT-5F** (**3**) assembles via an isodesmic mechanism, whereas **BTT** (**4**) assembles via a cooperative mechanism.¹³ Since isodesmic supramolecular polymers are sensitive to concentration²¹ the degree of dilution has to be carefully considered for H/D exchange. UV spectroscopy experiments showed that **BTT-5F** (**3**) requires a concentration higher than 25 μM to remain polymerized (Figure S8, ESI[†]). Thus, in this case, a 10x dilution from 500 to 50 μM was required for the HDX-MS experiments. We also selected a 10x dilution from 500 to 50 μM in the case of **BTT** (**4**).

BTT-5F (**3**) and **BTT** (**4**) molecules have nine labile hydrogen atoms: three alcohol hydrogen atoms at the periphery, three NH atoms of the *L*-phenylalanine derivatives and three NH atoms next to the

benzotrithiophene core (Figure 4(A)). Interestingly, for **BTT-5F** (**3**) the fully deuterated **BTT-5F9D** is the major isotope distribution observed after only 3 min of H/D exchange (Figure S9, ESI[†]). Only a small peak is observed for **BTT-5F3D** and this peak does not disappear after 24 h. This can be explained by the formation of a more stable conformation or by the presence of a small impurity in the sample, but the exact origin of this peak is currently unknown. The fast exchange of the amide hydrogen atoms of **BTT-5F** (**3**) is not caused by a too low concentration, since UV spectroscopy experiments indicate that HDX-MS experiments are conducted at a concentration where the monomers are sufficiently aggregated (Figure S8, ESI[†]). Additionally, the ESI-MS spectrum in D_2O does not completely overlap with the reference spectrum of the molecularly dissolved state (Figure S9, ESI[†]), indicating that the molecules are still assembled after dilution.

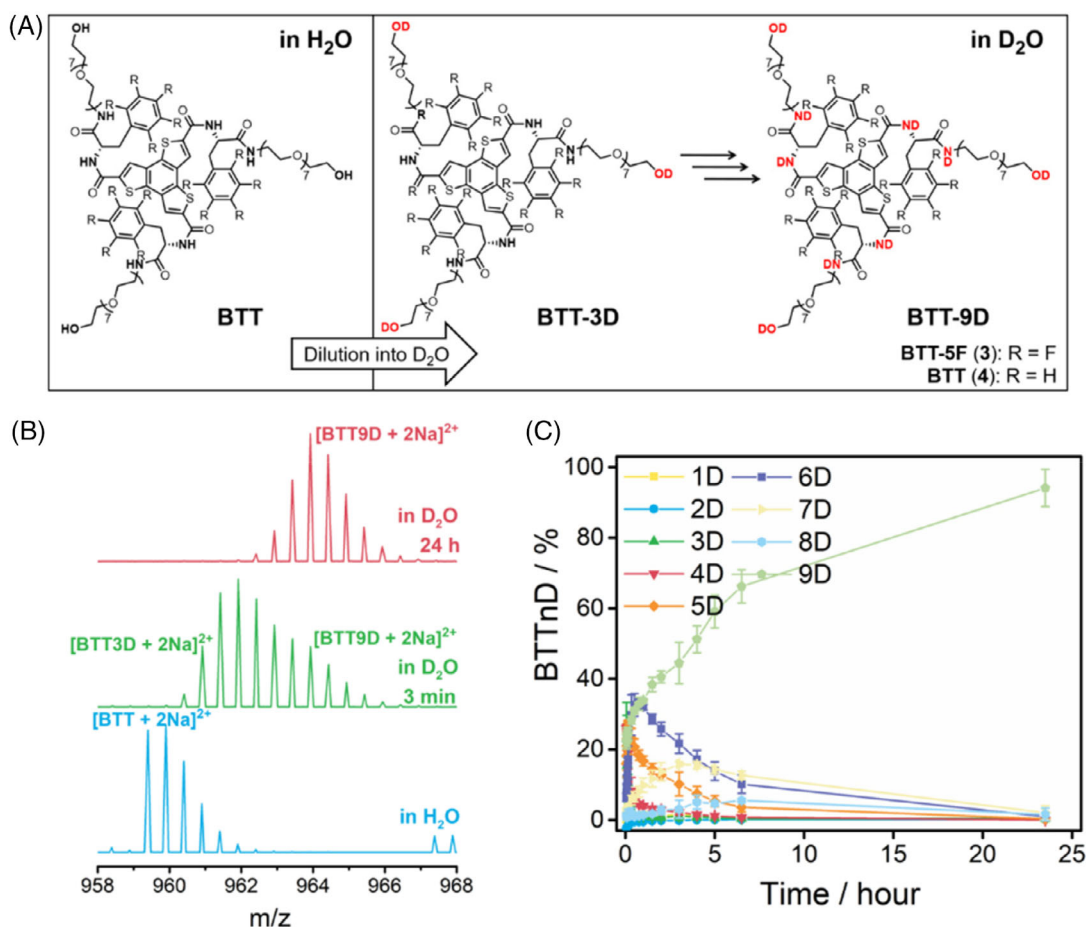


FIGURE 4 HDX-MS experiment of **BTT-5F (3)** and **BTT (4)**. (A) Schematic representation of the HDX-MS process of the BTT molecules, including the chemical structures of BTT analogues before and after dilution. (B) ESI-MS spectra of the doubly charged ions of **BTT (4)** after 10x dilution of a $c = 500 \mu\text{M}$ sample. The sample was diluted into H_2O or D_2O . (C) The percentage of the different deuterated analogues of **BTT (4)** as a function of time after the dilution of a $c = 500 \mu\text{M}$ sample 10x into D_2O ($T = \text{room temperature}$). The symbols represent the average and the error bars the standard deviation calculated from three independent measurements. The lines are added to guide the eye. BTT, benzotrithiophene; HDX-MS, hydrogen/deuterium exchange mass spectrometry [Color figure can be viewed at wileyonlinelibrary.com]

In contrast to **BTT-5F (3)**, the NH atoms of **BTT (4)** do not immediately exchange into NDs. For **BTT (4)**, we expect BTT3D with all the three peripheral hydroxyl hydrogens replaced by deuterium, to be present immediately after 10x dilution into D_2O , while BTT9D is present when complete H/D exchange is achieved (Figure 4(A)). Indeed, after 24 h, BTT9D dominates, indicating that almost all hydrogen atoms have exchanged (Figure 4(B), Figure S10, ESI⁺). Interestingly, BTT4D is the most prominent species after 3 min of exchange in D_2O and many other intermediates between BTT3D and BTT9D can be observed. Calculating and plotting the percentage of deuterated species versus time shows that the contribution of the deuterated intermediates first increases. Similar to **BU (2)**, the more deuterium atoms are exchanged, the longer it takes to reach the maximum

percentage (Figure 4(C)). Even after 7 h of H/D exchange, there is a significant percentage of **BTT (4)** molecules of which the core amide hydrogen atoms have only been partly exchanged for deuterium atoms, which is remarkably different from the other molecules studied here. The HDX-MS experiments presented above indicate that there are noticeable differences in the exchange dynamics of the different compounds. The compound **BTT-5F (3)**, which has an isodesmic formation mechanism, shows an immediate exchange of all labile hydrogens. **BTA (1)**, **BU (2)** and **BTT (4)**, which all show cooperative formation mechanisms, require longer times for the labile NHs to exchange. The implications of those differences in the mechanism of formation and differences in the formed morphologies on the mechanism of H/D exchange will be discussed in the next section.

2.3 | Consequences of the mechanism of exchange on the HDX dynamics in supramolecular polymers

The time-dependent HDX-MS experiments shown in Figures 2, 3(C), and 4(C) permit to extract information about the mechanism of H/D exchange. The peripheral hydrogen atoms are immediately exchanged for deuterium atoms due to their constant accessibility to the solvent, whereas two mechanism can cause the conversion of labile hydrogen atoms buried in the hydrophobic pocket. First, a D₂O molecule can penetrate into the hydrophobic parts of the supramolecular polymers and exchange the NHs in theory one at the time, forming intermediate deuterated species. Second, the release of a supramolecular monomer into the solution results in the exchange of all labile NHs to NDs at the same time. This last process has previously been shown for **BTA (1)** to occur during several hours with super resolution microscopy.²³ Obviously, these two exchange mechanisms cannot be completely isolated from each other because the monomers exchanged by D₂O penetration can also be released later via the monomer releasing mechanism. Since we now have access to the percentage of all deuterated species during HDX as a function of time, we can elucidate which process may be dominant in each of the systems studied. In addition, we can evaluate how the mechanism of formation and the nature of morphologies formed affect the HDX kinetic profile.

For **BTA (1)**, analysis of the percentage of BTA4D and BTA5D shows that in the first few minutes there is around 7–12% of BTA4D and BTA5D (Figure S5a, ESI[†]). The percentage of BTA4D decreases within the first 20 min of the experiment from 7.4 to 0.1%, but the percentage of BTA5D increases in the first 10 min to 11.5% before it decreases in the following 35 min to 2.0%. From this, we conclude that D₂O molecules penetrate into some less ordered assemblies in the first hour, leading to the exchange of one amide hydrogen atom at a time until these assemblies are fully deuterated. After 1 h the percentage of BTA4D and BTA5D is constant and negligible, suggesting that the part of the sample that undergoes H/D exchange via solvent molecule penetration has completely exchanged and that the remainder of the formation of BTA6D occurs via a monomer-release mechanism. The constant presence of trace amounts of BTA2D and BTA5D after 1 h is attributed to an underestimation of the percentage of H₂O in the sample during the calculations. In addition, the percentage of BTA6D rapidly increases in the first hour and then the increase levels off. After 24 h of HDX, 59% of the BTAs are BTA6D. After 72 h, this percentage increased to 70% and the H/D exchange was still not complete (Figure S5b, ESI[†]). This

implicates that part of the BTA assemblies does not easily releases its monomers into the solution. **BTA (1)** assembles into long one-dimensional assemblies as shown with cryoTEM (Figure 5(A)). Recently, we found that double helices are present in the sample next to other supramolecular structures.⁴⁷ We hypothesize that the formation of a double helix stabilizes the interactions between the BTAs, which would prevent them from moving into the solvent and therefore a slowing down of the H/D exchange of the core amides can occur.

In the case of **BU (2)** the high percentage of intermediate species BU3D, BU4D and BU5D over a long period shows that solvent penetration has a significant contribution to the H/D exchange. The extended time needed to exchange all hydrogen atoms of these intermediates indicates that there is a difference in solvent accessibility between the molecules within the assemblies. It is known that bisurea bola-amphiphiles are able to form wormlike micelles via the aggregation of 9–10 ribbons into one bundled structure.⁴⁸ CryoTEM images show that **BU (2)** assembles into elongated supramolecular assemblies with a diameter of roughly 6 nm (Figure 5(B)). This value is in agreement with the diameter of similar compounds that have been reported to consist of multiple ribbons,⁴⁸ confirming that **BU (2)** adopts the same morphology. Ribbons that are situated more on the inside of the bundles

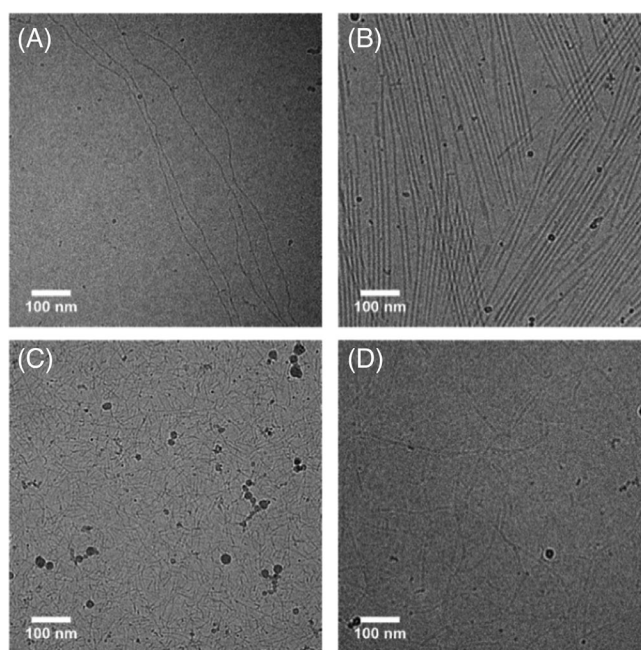


FIGURE 5 CryoTEM images of **BTA (1)** (A), **BU (2)** (B), **BTT-5F (3)** (C) and **BTT (4)** (D) in water ($c = 500 \mu\text{M}$, scale bar is 100 nm). The dark spherical objects are ice contamination. BU, bisurea amphiphile; BTA, benzene-1,3,5-tricarboxamides; BTT, benzotrithiophene; cryoTEM, cryogenic transmission electron microscopy

will take longer to have their hydrogen atoms exchanged than ribbons that are closer to the surface of the assemblies, resulting in a longer period in which the solvent penetration mechanism can be observed. Previous sonication experiments confirm that the supramolecular assemblies are reversible and that molecules can move between assemblies.⁵¹ Initially, the H/D exchange of **BU** (**2**) is dominated by the penetration of D₂O. After 5 h, the monomer-release mechanism is the main mechanism for H/D exchange.

BTT-5F (**3**) assembles into short fibrillar supramolecular polymers in water as shown with cryoTEM (Figure 5 (C)). However, the H/D exchange seems to be very fast and already after 3 min BTT-5F9D is the dominant species (Figure S9b, ESI†). Previous MD simulations revealed that the main interaction in the **BTT-5F** (**3**) assemblies is the hydrophobic interaction between the L-pentafluorophenylalanines instead of the hydrogen bonds between the core amides.³⁸ From these experiments, it was concluded that **BTT-5F** (**3**) molecules do not pack tightly, leading to the rapid dynamics of monomer releasing and/or the easy penetration of water molecules into the polymers. Thus, the exchange of NHs to NDs is fast.

CryoTEM images of **BTT** (**4**) (Figure 5(D)) show that the molecules assemble into longer supramolecular polymers than **BTT-5F** (**3**) (Figure 5(C)). According to MD simulations, the main interactions in **BTT** (**4**) are between amides of the benzotrithiophene cores.¹³ These cooperative interactions make the assemblies of **BTT** (**4**) more ordered, resulting in a slower exchange as compared to **BTT-5F** (**3**). Interestingly, the H/D exchange of the amides of **BTT** (**4**) is fast and significantly driven by solvent penetration as inferred from the high percentages of BTT4D, BTT5D, BTT6D, BTT7D, and BTT8D. This fast exchange and solvent penetration may be explained by the lack of a secondary structure in **BTT** (**4**) assemblies, which do not seem to show the double helix structure as found for **BTA** (**1**).

The kinetic profiles of the HDX-MS experiments of the three cooperatively formed supramolecular assemblies can now be compared. To minimize the effects of the different exchange mechanisms and intermediates, only the percentage of molecules with all hydrogen atoms exchanged are compared in Figure 6. Although the initial increase in BTA6D is fast, the rate of increase levels off after a few hours and only 59.4% of the BTAs are fully exchanged after 24 h. The percentage of BU6D initially increases less rapidly than that of BTA6D, but the fast exchange is maintained longer, resulting in an average of 78.6% of BU6D after 24 h. The percentage of BTT9D shows the most constant increase of all supramolecular assemblies and after 23.5 h the percentage of fully deuterated molecules is 94.2%, thereby surpassing the

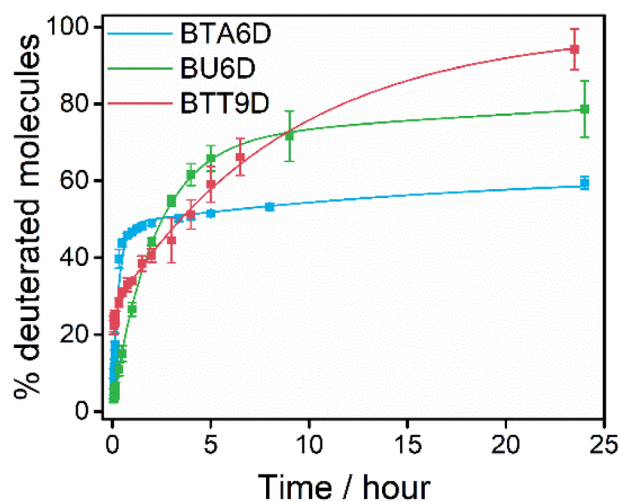


FIGURE 6 The percentage of fully deuterated **BTA** (**1**), **BU** (**2**) and **BTT** (**4**) as a function of time. All HDX-MS experiments were started with a $c = 500 \mu\text{M}$ sample in H₂O. The samples for **BTA** (**1**) and **BU** (**2**) were diluted 100x into D₂O and the sample of **BTT** (**4**) was diluted 10x into D₂O ($T = \text{room temperature}$). The squares represent the average and the error bars the standard deviation calculated from three independent measurements. The lines represent a bi-exponential growth function that was used to fit the data. BU, bis-urea amphiphile; BTA, benzene-1,3,5-tricarboxamides; BTT, benzotrithiophene; HDX-MS, hydrogen/deuterium exchange mass spectrometry [Color figure can be viewed at wileyonlinelibrary.com]

percentage of BTA6D and BU6D obtained after 24 h. From these results, it can be concluded that **BTA** (**1**) forms assemblies that are the most stable, whereas the assemblies of **BTT** (**4**) are the least stable.

Interestingly, the increase in the percentage of fully deuterated molecules of all supramolecular assemblies can be described with a bi-exponential growth function using a fast and a slow contribution. The rate of exchange can be quantified by a rate constant, k , and a relative distribution (see ESI† Section 5 for details on the fits). BTT9D has the highest rate constants in both regimes, whereas BU6D has the lowest rate constants. The large contribution of the fast exchange of BU6D results in more exchange in assemblies of **BU** (**2**) than in assemblies of **BTA** (**1**) over time. The fast exchange of BTT9D only has a small contribution and therefore the percentage of completely deuterated molecules is lowest for BTT9D in the first 10 h. From the bi-exponential fit it can be concluded that **BTA** (**1**) will never have all its hydrogen atoms replaced for deuterium atoms, resembling very stable amyloid fibrils.^{41,42} This very stable component of the assemblies of **BTA** (**1**) might be caused by the double helix structure,⁴⁷ but the exact origin is still under investigation.

3 | CONCLUSIONS

HDX-MS is a very attractive method for the characterization of dynamic supramolecular polymers in water, and only needs a minimal perturbation of the molecular structure of interest. We first confirmed some experimental aspects to obtain the most reliable results. Our results show that the application of MALDI is fundamentally limited because of the significant back-exchange reactions during the ionization process and therefore ESI-MS is the method of choice. No considerable differences in the polymer dynamics were observed whether the sample was diluted 100 times or 10 times into D₂O as long as the trace amount of H₂O was taken into account. Finally, we confirmed that the begin and end concentration are not of influence as long as both are above the CAC of the supramolecular building blocks.


The usefulness of HDX-MS is further demonstrated by applying this technique to different types of supramolecular polymers with different assembly mechanisms, one BTA-based, one BU-based and two BTT-based. These HDX-MS experiments not only monitored the movement of monomers between assemblies, but also revealed that solvent molecules can penetrate the supramolecular polymers because of imperfect stacking of the molecules. This solvent penetration allowed us to extract information about the internal structure of the supramolecular assemblies that was otherwise hidden. HDX-MS is an important complement to many techniques widely used for the characterization of supramolecular systems in water. Instead of providing information about the global polymer structure, HDX-MS allows insights into the internal order of structurally diverse samples. Furthermore, HDX-MS can also be extremely useful to assist in the rational design of building blocks able to form supramolecular polymers in water. These results demonstrate that the structure, self-assembly mechanism and dynamics of supramolecular polymers are not independent variables and should be evaluated simultaneously.

ACKNOWLEDGMENTS

René Lafleur and Lorenzo Albertazzi are gratefully acknowledged for initial discussions. The research in Eindhoven is supported by the Dutch Ministry of Education, Culture and Science (Gravity program 024.001.035) and the European Research Council (H2020-EU.1.1., SYNMAT project, ID 788618). Marcos Fernández-Castaño Romera was financially supported by the Marie Curie FP7 SASSYPOL ITN program (No. 607602). Miguel Garcia-Iglesias acknowledges financial support from MINECO, Spain (IJCI-2015-252389).

ORCID

Miguel Garcia-Iglesias  <https://orcid.org/0000-0001-6359-9020>

Marcos Fernández-Castaño Romera  <https://orcid.org/0000-0002-4899-0766>

Rint P. Sijbesma  <https://orcid.org/0000-0002-8975-636X>

E. W. Meijer  <https://orcid.org/0000-0003-4126-7492>

Anja R. A. Palmans  <https://orcid.org/0000-0002-7201-1548>

REFERENCES

- [1] B. N. S. Thota, L. H. Urner, R. Haag, *Chem. Rev.* **2016**, *116*, 2079.
- [2] H. L. K. Fu, C. Po, S. Y. L. Leung, V. W. W. Yam, *ACS Appl. Mater. Interfaces* **2017**, *9*, 2786.
- [3] Y. Loo, S. Zhang, C. A. E. Hauser, *Biotechnol. Adv.* **2012**, *30*, 593.
- [4] E. Krieg, M. M. C. Bastings, P. Besenius, B. Rybtchinski, *Chem. Rev.* **2016**, *116*, 2414.
- [5] K. Petkau-Milroy, M. H. Sonntag, L. Brunsveld, *Chem. Eur. J.* **2013**, *19*, 10786.
- [6] M. H. Bakker, R. E. Kieltyka, L. Albertazzi, P. Y. W. Dankers, *RSC Adv.* **2016**, *6*, 110600.
- [7] G. A. Silva, C. Czeisler, K. L. Niece, E. Beniash, D. A. Harrington, J. A. Kessler, S. I. Stupp, *Science* **2004**, *303*, 1352.
- [8] W. E. M. Noteborn, V. Saez Talens, R. E. Kieltyka, *ChemBioChem* **2017**, *18*, 1995.
- [9] S. I. Stupp, *Nano Lett.* **2010**, *10*, 4783.
- [10] B. Rybtchinski, in *Hierarchical Macromol. Struct. 60 Years after Staudinger Nobel Prize II* (Ed: V. Percec), Springer International Publishing, Cham **2013**, p. 363.
- [11] J. Boekhoven, S. I. Stupp, *Adv. Mater.* **2014**, *26*, 1642.
- [12] R. Dong, Y. Zhou, X. Huang, X. Zhu, Y. Lu, J. Shen, *Adv. Mater.* **2015**, *27*, 498.
- [13] N. M. Casellas, S. Pujals, D. Bochicchio, G. M. Pavan, T. Torres, L. Albertazzi, M. Garcia-Iglesias, *Chem. Commun.* **2018**, *54*, 4112.
- [14] C. Rest, M. J. Mayoral, K. Fucke, J. Schellheimer, V. Stepanenko, G. Fernández, *Angew. Chem., Int. Ed.* **2014**, *53*, 700.
- [15] F. García, L. Sánchez, *Chem. Eur. J.* **2010**, *16*, 3138.
- [16] D. Straßburger, N. Stergiou, M. Urschbach, H. Yurugi, D. Spitzer, D. Schollmeyer, E. Schmitt, P. Besenius, *ChemBioChem* **2018**, *19*, 912.
- [17] S. S. Lee, T. Fyrner, F. Chen, Z. Álvarez, E. Sleep, D. S. Chun, J. A. Weiner, R. W. Cook, R. D. Freshman, M. S. Schallmo, K. M. Katchko, A. D. Schneider, J. T. Smith, C. Yun, G. Singh, S. Z. Hashmi, M. T. McClendon, Z. Yu, S. R. Stock, W. K. Hsu, E. L. Hsu, S. I. Stupp, *Nanotechnol.* **2017**, *12*, 821.
- [18] K. Petkau-Milroy, M. H. Sonntag, A. H. A. M. Van Onzen, L. Brunsveld, *J. Am. Chem. Soc.* **2012**, *134*, 8086.
- [19] J. P. Patterson, Y. Xu, M. A. Moradi, N. A. J. M. Sommerdijk, H. Friedrich, *Acc. Chem. Res.* **2017**, *50*, 1495.
- [20] H. Weissman, B. Rybtchinski, *Curr. Opin. Colloid Interface Sci.* **2012**, *17*, 330.
- [21] T. F. A. De Greef, M. M. J. Smulders, M. Wolffs, A. P. H. J. Schenning, R. P. Sijbesma, E. W. Meijer, *Chem. Rev.* **2009**, *109*, 5687.

- [22] J. H. Ortony, C. J. Newcomb, J. B. Matson, L. C. Palmer, P. E. Doan, B. M. Hoffman, S. I. Stupp, *Nat. Mater.* **2014**, *13*, 812.
- [23] L. Albertazzi, D. van der Zwaag, C. M. A. Leenders, R. Fitzner, R. W. van der Hofstad, E. W. Meijer, *Science* **2014**, *344*, 491.
- [24] L. Albertazzi, F. J. Martinez-Veracoechea, C. M. A. Leenders, I. K. Voets, D. Frenkel, E. W. Meijer, *Proc. Natl. Acad. Sci.* **2013**, *110*, 12203.
- [25] K. Petkau-Milroy, D. A. Uhlenheuer, A. J. H. Spiering, J. A. J. M. Vekemans, L. Brunsveld, *Chem. Sci.* **2013**, *4*, 2886.
- [26] S. I. S. Hendrikse, S. P. W. Wijnands, R. P. M. Lafleur, M. J. Pouderoijen, H. M. Janssen, P. Y. W. Dankers, E. W. Meijer, *Chem. Commun.* **2017**, *53*, 2279.
- [27] X. Lou, R. P. M. Lafleur, C. M. A. Leenders, S. M. C. Schoenmakers, N. M. Matsumoto, M. B. Baker, J. L. J. van Dongen, A. R. A. Palmans, E. W. Meijer, *Nat. Commun.* **2017**, *8*, 15420.
- [28] T. E. Wales, J. R. Engen, *Mass Spectrom. Rev.* **2006**, *25*, 158.
- [29] L. Konermann, D. A. Simmons, *Mass Spectrom. Rev.* **2003**, *22*, 1.
- [30] S. W. Englander, *J. Am. Soc. Mass Spectrom.* **2006**, *17*, 1481.
- [31] L. Konermann, J. Pan, Y.-H. Liu, *Chem. Soc. Rev.* **2011**, *40*, 1224.
- [32] A. J. Percy, M. Rey, K. M. Burns, D. C. Schriemer, *Anal. Chim. Acta* **2012**, *721*, 7.
- [33] J. R. Engen, T. E. Wales, *Annu. Rev. Anal. Chem.* **2015**, *8*, 127.
- [34] S. W. Englander, *Annu. Rev. Biophys. Biomol. Struct.* **2000**, *29*, 233.
- [35] A. N. Hoofnagle, K. A. Resing, N. G. Ahn, *Annu. Rev. Biophys. Biomol. Struct.* **2003**, *32*, 1.
- [36] V. Katta, B. T. Chait, *Rapid Commun. Mass Spectrom.* **1991**, *5*, 214.
- [37] L. Konermann, S. Vahidi, M. A. Sowole, *Anal. Chem.* **2014**, *86*, 213.
- [38] W. Hu, B. T. Walters, Z. Y. Kan, L. Mayne, L. E. Rosen, S. Marqusee, S. W. Englander, *Proc. Natl. Acad. Sci. U. S. A.* **2013**, *110*, 7684.
- [39] R. E. Iacob, J. R. Engen, *J. Am. Soc. Mass Spectrom.* **2012**, *23*, 1003.
- [40] D. L. Smith, Y. Deng, Z. Zhang, *J. Mass Spectrom.* **1997**, *32*, 135.
- [41] N. Carulla, M. Zhou, M. Arimon, M. Gairi, E. Giralt, C. V. Robinson, C. M. Dobson, *Proc. Natl. Acad. Sci.* **2009**, *106*, 7828.
- [42] N. Carulla, G. L. Caddy, D. R. Hall, J. Zurdo, M. Gairi, M. Feliz, E. Giralt, C. V. Robinson, C. M. Dobson, *Nature* **2005**, *436*, 554.
- [43] H. D. F. Winkler, E. V. Dzyuba, C. A. Schalley, *New J. Chem.* **2011**, *35*, 529.
- [44] Z. Qi, C. Schlaich, C. A. Schalley, *Chem. Eur. J.* **2013**, *19*, 14867.
- [45] L. Cera, C. A. Schalley, *Chem. Soc. Rev.* **2014**, *43*, 1800.
- [46] C. M. A. Leenders, L. Albertazzi, T. Mes, M. M. E. Koenigs, A. R. A. Palmans, E. W. Meijer, *Chem. Commun.* **2013**, *49*, 1963.
- [47] R. P. M. Lafleur, S. Herziger, S. M. C. Schoenmakers, A. D. A. Keizer, J. Jahzerah, B. N. S. Thota, L. Su, P. H. H. Bomans, N. A. J. M. Sommerdijk, A. R. A. Palmans, R. Haag, H. Friedrich, C. Böttcher, E. W. Meijer, *J. Am. Chem. Soc.* **2020**, *142*, 17644. .
- [48] M. Fernandez-Castano Romera, R. P. M. Lafleur, C. Guibert, I. K. Voets, C. Storm, R. P. Sijbesma, *Angew. Chem. Int. Ed.* **2017**, *56*, 8771.
- [49] R. P. M. Lafleur, X. Lou, G. M. Pavan, A. R. A. Palmans, E. W. Meijer, *Chem. Sci.* **2018**, *9*, 6199.
- [50] N. Chebotareva, P. H. H. Bomans, P. M. Frederik, N. A. J. M. Sommerdijk, R. P. Sijbesma, *Chem. Commun.* **2005**, 4967.
- [51] M. Fernández-Castaño Romera, X. Lou, J. Schill, G. Ter Huurne, P. P. K. H. Franssen, I. K. Voets, C. Storm, R. P. Sijbesma, *J. Am. Chem. Soc.* **2018**, *140*, 17547.

SUPPORTING INFORMATION

Additional supporting information may be found online in the Supporting Information section at the end of this article.

How to cite this article: Lou X, Schoenmakers SMC, van Dongen JLJ, et al. Elucidating dynamic behavior of synthetic supramolecular polymers in water by hydrogen/deuterium exchange mass spectrometry. *J Polym Sci.* 2021;59:1151–1161. <https://doi.org/10.1002/pol.20210011>